J. Fluid Mech. (1967), *vol.* 28, *part* 1, *pp.* 153–175
Printed in Great Britain

Turbulence measurements with inclined hot-wires

Part 1. Heat transfer experiments with inclined hot-wire

By F. H. CHAMPAGNE†,
Department of Chemical Engineering, University of Washington
and Boeing Scientific Research Laboratories

C. A. SLEICHER
Department of Chemical Engineering, University of Washington

AND O. H. WEHRMANN
Boeing Scientific Research Laboratories

(Received 20 June 1966)

The measurement of the turbulent shear stresses and normal and bi-normal intensities with a hot-wire anemometer requires that the directional sensitivity of the hot-wire be known. Normal component or cosine law cooling is generally assumed, although for finite wire lengths the non-uniform wire temperature must cause a deviation from the cosine law.

Careful heat transfer measurements from wires inclined and normal to the flow were taken for several values of the Reynolds number, the length-to-diameter ratio of the wire, the overheat ratio and for several support configurations. All experiments were performed in air at low subsonic velocities, i.e. $M < 0{\cdot}1$. The measurements indicate that the heat loss from an inclined wire is larger than that from a wire normal to the flow with the same normal component of velocity. The data were correlated by

$$U_E^2(\alpha) = U^2(0)\,(\cos^2\alpha + k^2\sin^2\alpha),$$

where $U_E(\alpha)$ is the effective cooling velocity at the angle α between the normal to the wire and the mean flow direction and $U(0)$ is the velocity at $\alpha = 0$. The value of k was found to depend primarily upon the length-to-diameter ratio (ℓ/d) of the wire. For platinum wires k is approximately 0·20 for $\ell/d = 200$, decreases with increasing ℓ/d, and becomes effectively zero at $\ell/d = 600$.

To aid in interpreting the heat transfer data, measurements of the temperature distribution along inclined and normal wires were made with a high sensitivity infra-red detector coupled to a high resolution microscrope with reflective optics. The measurements indicate that inclined wires and normal wires have nearly identical end conduction losses, although the temperature distribution on an inclined wire is slightly asymmetrical. Therefore, the deviation from the cosine law is caused by an increase in the convection heat loss, and this increase is attributed to the tangential component of velocity.

† Present address: Boeing Scientific Research Laboratories, Seattle, Washington.

1. Introduction

The measurement of the turbulent shear stresses and normal and bi-normal turbulent intensities with a hot-wire anemometer requires that the directional sensitivity of the hot-wire be known. The directional sensitivity is generally assumed to follow normal component cooling or the 'cosine law', although for finite wire lengths the non-uniform wire temperature may cause a deviation from the 'cosine law'. Normal component cooling refers to the assumption that the rate of heat transfer from a hot-wire depends on the flow field only through the

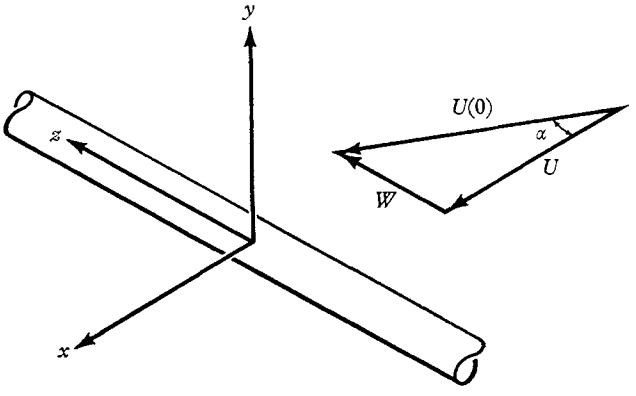

FIGURE 1. Sketch showing co-ordinate system used.

normal component of the velocity across the wire. This component is given by $U(0)\cos\alpha$, where $U(0)$ is the magnitude of the velocity and α is the angle between the normal to the wire and the flow direction, as shown in figure 1.

The directional sensitivity of a hot-wire may be obtained by direct calibration, but to do so with sufficient accuracy is an arduous task, and at times experimental conditions may render it impossible. Thus a formulation to relate the effective cooling velocity detected by the wire to the mean velocity of the stream and the angle of inclination is desirable.

Prandtl (1946), Jones (1947) and Sears (1948) established that for laminar flow past an infinitely long cylinder oblique to a uniform velocity field, the two velocity components in a plane normal to the axis of the cylinder are independent of the axial component. If the cylinder is heated uniformly along its axis, consideration of the energy equation shows that the rate of heat loss per unit length depends only on the normal velocity components. From these facts the cosine law of directional sensitivity can be established for an infinitely long hot-wire anemometer, and this result is generally assumed to apply to wires of finite length. Schubauer & Klebanoff (1946) experimentally tested the validity of the cosine law and concluded that it held for finite wires for angles of yaw less than 70°. Thus the data could be correlated with the Reynolds number based on the normal component of the velocity to the wire as follows:

$$N = A + B(R\cos\alpha)^{\frac{1}{2}}, \tag{1}$$

where N is the Nusselt number and R the Reynolds number. Newman & Leary (1950) concluded that the wire responded to

$$N = A + BR^{\frac{1}{2}}(\cos\alpha)^n, \tag{2}$$

with $n = 0{\cdot}457$, while Sandborn & Laurence (1955) found that the exponent n varied with each wire tested. The latter made extensive measurements at fixed subsonic Mach numbers and angles of yaw up to 90°, i.e. the wire parallel to the mean flow direction. It was found that the effect of length-to-diameter ratio, ℓ/d, on the rate of heat loss from wires normal to the flow could be eliminated by end-loss corrections. The corrections were assumed to hold for yawed wires also, which is equivalent to the assumption that the end conduction loss to the prongs is independent of the angle of yaw. The authors proposed an empirical relation of the form

$$N = (A + B(R\cos\alpha)^{\frac{1}{2}})\cos\alpha + (C + D(R\sin\alpha)^{\frac{1}{2}})\sin\alpha, \tag{3}$$

which is based on the weighted addition of the heat losses of normal and parallel wires. Since systematic deviations were observed, however, a need for a more accurate equation was indicated.

Kronauer (1953) suggested that the deviation from the cosine law is dependent on the length-to-dimeter ratio of the wire and substantially independent of the Reynolds number. Kronauer expressed his results in the form

$$U_E(\alpha) = U(0)\cos\alpha + 1{\cdot}2(d/\ell)^{\frac{1}{2}}\sin^2\alpha, \tag{4}$$

where U_E is the effective cooling velocity detected by the wire.

Hinze (1959), and more recently, Webster (1962), suggested the following expression for the effective cooling velocity:

$$U^2(\alpha) = U^2(0)\,(\cos^2\alpha + k^2\sin^2\alpha). \tag{5}$$

Hinze reported that k increases with decreasing velocity and ranges from 0·1 to 0·3. Webster determined k to be 0·20, but there was considerable scatter in his values. His results show no systematic dependence of k on length-to-diameter ratio.

A theoretical analysis of the deviation from the cosine law was made by Corrsin (1963). The analysis, however, assumes the cosine law in the calculation of the convection loss term. As a consequence the analysis gives a correction to the cosine law which arises only from the variation of end conduction losses with angle of inclination.

Delleur (1964) stated that for angles of yaw less than 70° the cosine law is valid, but for angles greater than 70° the effective cooling velocity is given by (5) with $k = 0{\cdot}14$. No dependence on length-to-diameter ratio or the Reynolds number was reported. Chu (1964) also reported results which indicate no appreciable deviation from the cosine law. He used linearized constant-temperature operation for his experiments, however, and the noise in the electronics may have masked any deviations from the cosine law.

Davies & Fisher (1964) stated that their measurements are in good agreement with those obtained by Sandborn & Laurence. They also suggested that the end

conduction losses are dependent on the angle of yaw because of a possible shifting of the temperature maximum on the wire from its centre toward the downstream end. The resulting asymmetrical temperature distribution could alter the heat lost by conduction to both supports.

From the foregoing literature summary it is evident that there is considerable disagreement as to the directional sensitivity of a hot-wire and, therefore, to the accuracy of measurements made with wires oblique to the flow when cosine law cooling is assumed. The present investigation was undertaken to determine more accurately the directional sensitivity of a hot-wire and, moreover, to determine whether any observed deviations from normal component or cosine law cooling are caused by changes in the convection mode of heat loss or by changes in end conduction losses to the prongs.

2. Theoretical considerations

For an electrically heated cylinder placed in a steady uniform velocity field, the condition of thermal equilibrium requires that the heat generated is balanced by convection, conduction loss to the supports, and radiation. For Reynolds numbers and wire temperatures considered in the present investigation, the radiation heat loss amounts to about 0·005 % of the total and will be neglected. Thus, heat is lost only by convection and the conduction to the supports. The flow will be considered incompressible, since the Mach number is less than 0·1, and slip or Knudsen number effects will be neglected.

2.1. *Convective heat transfer from hot-wires*

In steady, uniform, isothermal flow, the rate of convective heat loss from a solid body depends on the flow velocity, the body geometry, the temperature difference between the body and the fluid, and the physical properties of the fluid. For a straight, circular cylinder, experimental and theoretical research (Corrsin 1963) has indicated that the dimensionless heat transfer coefficient can be correlated by

$$N = f(R, Pr, G, \ell/d, (T_m - T_a)/T_a, \alpha), \tag{6}$$

where Pr is the Prandtl number, G is the Grashof number, ℓ/d is the wire length-to-diameter ratio and $(T_m - T_a)/T_a$ is the mean overheat ratio of the wire. T_m and T_a are the mean wire temperature and ambient temperature, respectively. Ordinarily, a hot-wire is used under conditions in which buoyancy effects are negligible (e.g. Collis 1956), and hence G can be deleted from further consideration.

Many empirical relationships have been reported for the heat transfer from heated cylinders oblique to the flow. As already mentioned, however, these relationships differ with respect to ℓ/d and α dependency. The effects of α and ℓ/d on N are inter-related as will now be shown by extending Corrsin's (1963) analysis for an infinite cylinder to the case of a finite cylinder. Many investigators (Prandtl 1946; Jones 1947; Sears 1948) have shown that for laminar flow over an infinitely long cylinder inclined to a uniform velocity field, the two velocity components normal to the cylinder axis are independent of the axial component. This separation is usually referred to as the 'independence principle' (Sears 1954). In the

rectangular Cartesian co-ordinates shown in figure 1 the Navier–Stokes equations and continuity equation reduce to

$$\frac{\partial u}{\partial t}+u\frac{\partial u}{\partial x}+v\frac{\partial u}{\partial y}=-\frac{1}{\rho}\frac{\partial p}{\partial x}+\nu\left(\frac{\partial^2 u}{\partial x^2}+\frac{\partial^2 u}{\partial y^2}\right), \tag{7}$$

$$\frac{\partial v}{\partial t}+u\frac{\partial v}{\partial x}+v\frac{\partial v}{\partial y}=-\frac{1}{\rho}\frac{\partial p}{\partial y}+\nu\left(\frac{\partial^2 v}{\partial x^2}+\frac{\partial^2 v}{\partial y^2}\right), \tag{8}$$

$$\frac{\partial w}{\partial t}+u\frac{\partial w}{\partial x}+v\frac{\partial w}{\partial y}=\nu\left(\frac{\partial^2 w}{\partial x^2}+\frac{\partial^2 w}{\partial y^2}\right), \tag{9}$$

$$\frac{\partial u}{\partial x}+\frac{\partial v}{\partial y}=0. \tag{10}$$

For an infinite cylinder heated uniformly along z, the energy equation for an incompressible fluid with negligible viscous dissipation reduces to

$$\frac{\partial T}{\partial t}+u\frac{\partial T}{\partial x}+v\frac{\partial T}{\partial y}=\frac{\kappa}{\rho C_p}\left(\frac{\partial^2 T}{\partial x^2}+\frac{\partial^2 T}{\partial y^2}\right). \tag{11}$$

The temperature field is independent of the axial velocity component w, and so the convective heat loss rate per unit length depends only on the normal velocity components. Thus the cosine law can be established for an infinite wire. The relation for the Nusselt number therefore becomes

$$N=f(R\cos\alpha, Pr, (T_m-T_a)/T_a). \tag{12}$$

For the wires used in this study the length-to-diameter ratios varied from 200 to 600, so $\ell/d=O(10^2)$. Thus, it is reasonable to assume that the Navier–Stokes equations and continuity equation for the flow field around these wires reduce to the form for an infinite wire to a close approximation. The temperature along the wires of finite length, however, will not be uniform because of the end conduction losses. In this case, the $\partial(\ )/\partial z$ terms in the energy equation may not be negligible, and so the heat transfer will depend on the axial velocity component as well as the two components normal to the cylinder axis. The effective velocity causing the convective heat loss will, therefore, be some combination of the normal and tangential (axial) velocity components, which when added vectorially give (5), the equation given by Hinze (1959). The expression for the Nusselt number for a wire of finite length takes the form

$$N=f(R(\cos^2\alpha+k^2\sin^2\alpha)^{\frac{1}{2}}, Pr, (T_m-T_a)/T_a). \tag{13}$$

Comparison of this equation with (12) indicates that $k\to 0$ as $\ell/d\to\infty$. Thus k must depend on ℓ/d and the parameters that determine the temperature distribution along the wire, and the sensitivity to the tangential velocity component decreases as the ℓ/d ratio increases.

An inherent assumption in the above analysis is that the development of the w-component of velocity is complete well before $\ell/d=200$ on the finite wires. This assumption appears to be reasonable for the conditions of this study, i.e. Reynolds numbers in the range 5–30 and angles of inclination from 0° to about 60°. However, hydrodynamic end effects have been considered in the interpretation of our experimental results as a possible cause of deviation from the cosine law.

The possibility of obtaining solutions to (7)–(11) for the Reynolds numbers of interest is quite remote, especially since these equations are coupled with the equation governing the temperature distribution along the wire. Even if a solution could be obtained, it would not be valid near the wire ends where three-dimensional effects come into play. Therefore, an experimental approach based on the empirical relation (5) for the effective velocity was used to determine the effect of the tangential velocity component on the heat transfer from inclined wires.

2.2. *Wire temperature distribution equations*

The temperature distribution along the wire is determined by the heat generated in the wire, the convective heat loss, and the end conduction loss to the wire supports. Since the end supports are ordinarily much larger in diameter than the wire, they are assumed to be effectively at ambient temperature and cause the undesirable non-uniform temperature distribution along the wire. It should be emphasized that inclined wires will not be considered here because the convection loss term in this case would be unknown.

The differential equation governing the wire temperature distribution for a wire in a uniform, steady flow is given by (Corrsin 1963)

$$a\frac{d}{dz}\left(\kappa_w(\theta)\frac{d\theta}{dz}\right)+NI^2\rho_1(\theta)-\phi(U,\theta)=0, \tag{14}$$

where $\theta = T_w - T_a$, local wire-to-air temperature difference; $a = \pi d^2/4$, the wire cross-sectional area; κ_w = thermal conductivity of the wire material; I = current; ρ_1 = local resistance per unit length of wire material; ϕ = local convective heat loss rate per unit length.

The assumptions incorporated in (14) are: radiation heat loss is negligible, radial temperature gradients can be neglected (see King 1914), and ℓ/d is sufficiently large that the local convection heat loss depends only on the local wire-to-air temperature difference. Many investigators (King 1914; Betchov 1952; Davies & Fisher 1964; Schollmeyer 1965) have obtained solutions to special cases of (14), but for the sake of brevity these results will not be discussed here.

The following relations will be used for (14):

$$\left.\begin{aligned}\kappa_w &= \kappa_{wa}(1+\xi\theta),\\ \rho_1 &= \rho_{1a}(1+\alpha\theta+\beta\theta^2),\\ \phi(U,\theta) &= \rho_{1a}\alpha[A_a(1+a_1\theta)+B_a(1+b_1\theta)\,U^n]\theta.\end{aligned}\right\} \tag{15}$$

The expression for the convection loss term $\phi(U,\theta)$ is taken from Collis & Williams (1959). They obtained the values $\rho_{1a}\alpha A_a\ell = 0{\cdot}24$, $\rho_{1a}\alpha B_a\ell = 0{\cdot}56$ and $n = 0{\cdot}45$. This expression is valid for wires normal to the flow of air and for $0{\cdot}02 < R < 44$, which is the range of interest here. These results were obtained for wires with aspect ratios, ℓ/d, greater than 10^3 and cannot be applied to wires with $\ell/d \approx 2\times 10^2$, which are often used in turbulence measurements, because of three-dimensional effects. Collis (1956) states that the aspect ratio affects the value of the constants A and B but not n. This statement and the value of 0·45 for n were confirmed by

Champagne & Lundberg (1966). Therefore, the values of A_a and B_a were obtained experimentally for each wire for which a temperature distribution calculation was carried out. The end conduction loss, as determined from the temperature distribution, was accounted for in evaluating A_a and B_a.

If the relations (15) and $\eta = z/\ell$ and $\Theta = \theta/T_a$ are introduced into (14), the resulting equation is

$$(1+C_1\Theta)\frac{d^2\Theta}{d\eta^2}+C_1\left(\frac{d\Theta}{d\eta}\right)^2+C_2\Theta+C_3\Theta^2+C_4=0, \tag{16}$$

with

$$C_1 = \xi T_a,$$

$$C_2 = \frac{\rho_{1a}\alpha\ell^2}{a\kappa_{wa}}[NI^2-(A_a+B_a U^{0\cdot45})],$$

$$C_3 = \frac{\rho_{1a}\ell^2}{a\kappa_{wa}}[NI^2\beta T_a-\alpha(A_a a_1 T_a+B_a b_1 T_a U^{0\cdot45})],$$

$$C_4 = \frac{NI^2\ell^2\rho_{1a}}{a\kappa_{wa}T_a}.$$

For small enough overheat ratios (16) reduces to

$$d^2\Theta/d\eta^2+C_2\Theta+C_4=0, \tag{17}$$

the equation solved by King (1914). The boundary conditions in the case of a wire normal to the flow for both (16) and (17) are

$$\Theta(0)=\Theta_0, \quad \Theta'(\tfrac{1}{2})=0. \tag{18, 19}$$

The value of Θ_0 is commonly assumed to be zero, although Schollmeyer (1965) indicates $\Theta_0 > 0$ and that its value depends on the wire and end support materials.

To solve (17) let $C_5 = -C_2$, because $C_2 > 0$ for all the cases considered here. Then its solution subject to (18) and (19) is

$$\Theta(\eta) = (C_4/C_5-\Theta_0)[\tanh\tfrac{1}{2}C_5^{\frac{1}{2}}\sinh C_5^{\frac{1}{2}}\eta-\cosh C_5^{\frac{1}{2}}\eta]+C_4/C_5. \tag{20}$$

The non-linear equation (16) was solved numerically by using a sixteenth-order power series expansion technique which is described in detail by Champagne (1966). Later in the present paper the results are compared to measurements and discussed.

3. Experimental arrangement

3.1. *Heat transfer measurements*

The experiments were performed in the exit plane of a round, 1 in. diameter, jet in which the turbulence intensity was of the order of 0·1 %. The centres of all wires were located on the centre-line of the jet 0·15 in. downstream of the nozzle exit plane. Within $\frac{1}{4}$ in. of this point in any direction the static pressure was as close to ambient as we could measure, $\pm$ 0·005 in. of water. The radial velocity distribution over the inner 80 % of the jet radius was uniform within 2 parts in 10,000. The temperature of the air was maintained at a constant value to within

$\pm 0{\cdot}1$ °F during each run, and the air was cleaned with a Honeywell electrostatic precipitator which removed particles and hydrocarbons in the air as small as $0{\cdot}04\,\mu$ in diameter. The hot-wire probes were mounted on a device that permitted a probe to be inclined at any angle to the flow. Horizontal mounting of the hot-wires was used to maintain free convection effects, however small, independent of the angle of inclination of the wire. The hot-wire was viewed from above through a travelling microscope fitted with a protractor eyepiece which enabled the angle of the hot-wire with respect to a fixed datum to be determined to within 3 min of arc. The microscope assembly was out of the flow.

The hot-wires were operated in a bridge having high wattage components with low-temperature coefficients of resistance to minimize temperature-induced drift. A stabilized power supply was used to drive the bridge, and the bridge balance was maintained manually by varying the power input. Constant temperature operation was chosen to eliminate effects caused by changes of the overheat ratio as the wire was rotated.

The mean flow direction was determined by measuring the bridge voltage with the wire inclined at 5° intervals in the range $+20°$ to $-20°$ with respect to the fixed datum, which was preliminarily placed as close to 0° as could be determined by visual observation. The mean flow direction was determined to within $\pm 15'$ with this technique, and the 0° fixed datum was then locked at this position. This procedure was repeated for each run. Determination of the angle of yaw, α, is very critical in obtaining good data, for an error of 1° in α could cause an error of approximately 20 % in k.

It was desired to use only wires that were effectively straight when heated and placed in the flow field, and this presented a difficult problem for the longer wires. Platinum, tungsten, and platinum-plated tungsten wires with length-to-diameter ratios from 200 to 600 were used in the study. The tungsten wires had copper plating at the ends where the junction to the end supports was made. The platinum wires, however, were made from a smooth length of platinum wire, $5\,\mu$ in diameter, which was placed across the supports and soldered. To prevent wire sag caused by thermal elongation and the aerodynamic leading of the air-stream, a small amount of tension was placed on the wires by bending the prongs together very slightly before soldering. Although extreme care was taken in building the wires, many of the longer wires, $\ell/d > 300$, would sag when heated and placed in the flow, though they were straight and taut when unheated. The sagging wires were discarded.

The velocity range used was 7–35 m/s, although most of the runs were taken at $U_\infty = 35$ m/s. The overheat ratio, a_w, was kept at 0·80 for all the runs.

The data were taken after first establishing a temperature equilibrium in the flow system. The temperature was measured with a thermistor probe, which was mounted about $\frac{1}{2}$ in. under and ~ 3 in. behind the hot-wire. After the air temperature had stablized, a Pitot tube pressure measurement was made with an inclined alcohol manometer, after which the Pitot tube was removed from the flow field. The hot-wire was then placed in the flow at the 0° fixed datum angle, and the bridge was balanced. After a few minutes were allowed for the hot-wire to equilibrate, the bridge was balanced very carefully again. Then the voltage

across the bridge was read on a Hewlett–Packard Digital Voltmeter. The temperature of the air, the Pitot tube pressure reading, and the bridge voltage were simultaneously recorded. The wire was then inclined in 10–15° intervals in the range $-60°$ to $+60°$. Larger angles were not used to avoid any effects from the wake off the upstream wire support. Temperature readings were taken simultaneously with bridge voltage readings at each angle position. The wire was then positioned back at the fixed datum angle, and the bridge voltage, air temperature and pressure were recorded and compared with their counterparts at the beginning of the run to test for drift of any kind. If the bridge voltages did not agree to within ± 2 parts in 10^4, the run was normally rejected. The wire was subsequently calibrated using the Pitot tube and inclined manometer with the air temperature maintained to within $\pm 0{\cdot}1$ °F of the run temperature. The bridge voltages were converted to apparent velocities with the wire calibration, and then the best value of k in the sense of least squares was determined for each run.

3.2. *Temperature distribution measurements*

To determine whether the end conduction loss is a function of the angle of inclination of a wire, temperature distribution measurements along both normal and inclined wires were made. This required for the $5\,\mu$ or 0·0002 in. wire a technique which would have a spatial resolution of less than 0·0002 in. and which would not distort the temperature or flow fields around the wire nor the temperature of the wire itself. The technique that came closest to satisfying these requirements was the use of an infra-red radiometric microscope with a spatial resolution of 0·0003 in. and a temperature range from 25 to 650 °C. The thermal sensitivity of the infra-red detector could be considerably improved, however, by using reflective optics with a spatial resolution of 0·0008 in. This called for use of 0·001 in. diameter wires, which required scaling up the 0·0002 in. diameter hot-wire probes while maintaining geometric, dynamic and thermal similarity. This in turn required the ratio of the diameter of the support to the wire diameter, the length-to-diameter ratio, the Reynolds number, and the temperature loading to be the same for any two wires that were to be compared.

Sigmund Cohn pure reference grade platinum wire was used for all the 0·001 in. hot-wire probes. The diameter of the wire was not measured, and the manufacturer's specifications were accepted. The specifications were tested, however, by measuring the resistance of samples of the wire. The resistances were consistently within 1 % of a value calculated from resistivity data from the International Critical Tables. The end supports were made from pieces of nichrome wire approximately 0·25 in. long and 0·020 in. in diameter. They were soldered on the Disa 55 A 22 hot-wire probe, which was chosen for its low electrical resistance. These probe tips are shown in figures 2*a* and 2*b*. Care had to be taken in soldering the platinum wire to the end supports to assure that no solder or flux 'ran down' the wire. Solder or flux has a much higher emissivity than platinum and thus would give a higher voltage output reading, which would indicate a higher temperature than the actual wire temperature.

On some wires it was difficult to establish the exact position at which the wire

ended and the end prong began, for the solder tended to obscure this position. To establish the end conditions better and to simulate Wollaston wires, two special probes with $\ell/d \approx 200$ were constructed. They were made by tapering two pieces of 0·010 in. diameter platinum wire to approximately 0·005 in. and then drilling through each a 0·0028 in. axial hole. The holes were partially filled with solder, and the 0·010 in. ends were soldered to the end support with the smaller ends facing the opposite piece. The 1 mil wire was drawn through the holes by placing a hot soldering iron near the tip. This procedure was successful in preventing any contamination, such as solder or flux, from running down the wire. The end pieces were approximately 0·030 in. long. A photograph of one of the special ends is shown in figure 2*d*.

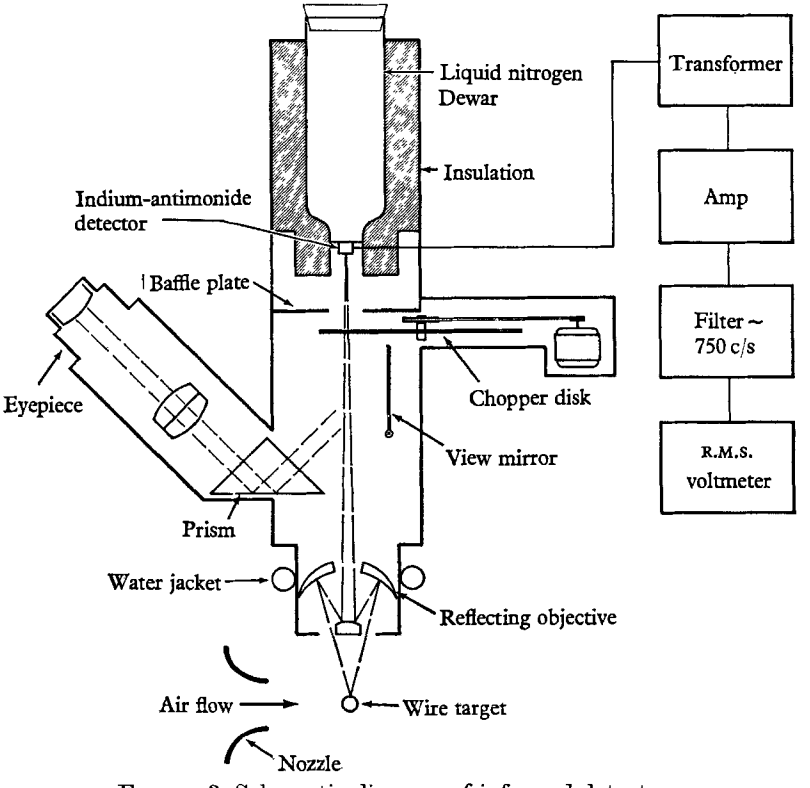

FIGURE 3. Schematic diagram of infra-red detector.

The Sierra-Philco Model 700*A* infra-red detector and associated equipment is shown schematically in figure 3. The unit is essentially a high resolution, high sensitivity infra-red detector. The detector system was calibrated directly, which eliminated the necessity of determining the emissivity and its dependence on temperature. A 0·001 in. thick platinum sheet was placed on a heater, and the heater was positioned under the detector. The temperature of the platinum sheet was measured with a platinum and platinum (13 %) rhodium thermocouple. The thermocouple was spot welded on the platinum sheet a few mils from the 6×10^{-7} sq.in. target area on which the detector was focused. The R.M.S. voltage

output of the detector unit was determined as a function of temperature from 20 °C to approximately 300 °C. This procedure was repeated on several different days, and the data were quite reproducible. The validity of using the calibration data in interpreting the data from the heated wires rests on the assumption that the emissivities of the platinum sheet and the wire are the same. A more detailed discussion of this matter and of other aspects of the calibration procedure are given by Champagne (1966).

The cold resistance of the wires was measured by two different instruments, and a current of 3·5 mA was normally used. One experiment was carried out to determine the effect of the amount of current used in making cold resistance measurements. Currents from 0·5 to 5 mA were used, and the resulting resistance values varied less than 1 %. The accuracy of resistance measurements was such that the overheat ratio could be determined to within ± 3 % for $a_w \approx 0{\cdot}8$ and on the order of ± 5 % for $a_w \approx 0{\cdot}50$.

A typical temperature distribution run proceeded as follows. A decade resistance box, accurate to 0·1 %, was used to balance the bridge at the desired resistance for the hot-wire and was then removed and the wire connected in the bridge. The wire was placed in the flow at the position previously described, and it was heated until the bridge was balanced. The focal length of the detector was sufficient to keep it out of the flow when focused on the wire. The wire was oriented perpendicular to the optical centreline of the microscope and the optics focused so that the wire could be scanned from one support to the other with only slight, if any, focusing adjustments. The wires were moved with an $X-Y$ micrometer unit. The unit had a 1 in. by 1 in. travel with an accuracy of $\pm 0{\cdot}0002$ in.

The static temperature of the stream and the total pressure were taken as in the heat transfer runs. The wire was first placed normal to the stream and the wire was scanned along its axis. R.M.S. voltage output readings were taken at 0·001 in. intervals near each end and at larger intervals near the centre of the wire. The voltage across the hot-wire was recorded, and the wire was then inclined at an angle, usually from 45° to 55°. The flow velocity was increased until the same voltage across the wire balanced the bridge, and this resulted in maintaining the normal component velocity essentially the same for both the inclined and normal wire. The foregoing procedure for obtaining the R.M.S. detector output voltage was repeated.

The mean wire temperature was determined by graphically integrating a plot of the wire temperature distribution. Comparison of this mean temperature with the resistance mean temperature, given in the next section, suggests that the calibration and operating procedures were adequate.

4. Results and discussion

4.1. *Heat transfer measurements*

Table 1 presents a summary of the heat transfer measurements, and some of the data are plotted in figures 4–6 as Nusselt number, N, verses $R^{\frac{1}{2}}(\cos\alpha)^{\frac{1}{2}}$ or R_N, the normal component Reynolds number. All physical properties of the air were evaluated at $\frac{1}{2}(T_m + T_a)$. To interpret these plots, it should be kept in mind that the

calibration data were taken at $\alpha = 0°$ by varying U_∞, while for the yawed wire U_∞ (or R) was held constant and α was varied. $(R)_\infty$ refers to the Reynolds number based on the free stream conditions. The deviations of the yawed wire data from the normal wire data, as shown in figures 4–6, give an indication of the magnitude

Run no.	$\sim U_\infty$ (m/s)	$(R)_\infty$	$\frac{d_{support}}{d_{wire}}$	Wire material†	ℓ/d	k
H1	35	11·7	25	Pt-Plated W	200	0·20 ± 0·04
H2	35	11·7	25	Pt-Plated W	200	0·20 ± 0·04
H3	35	11·7	50	W	375	0·12 ± 0·04
H4	35	11·7	12	Pt	450	0·09 ± 0·04
H5	35	11·7	12	Pt	450	0·10 ± 0·04
H6	35	11·7	12	Pt	200	0·22 ± 0·04
H7	35	11·7	10	Pt	240	0·18 ± 0·04
H8	7·5	2·5	10	Pt	240	0·16 ± 0·02
H9	35	10·0	17	W‡	566	0·06 ± 0·04
H10	35	11·7	10	Pt	600	0·00 ± 0·04
H11	35	11·7	50	Pt	200	0·23 ± 0·04
H12	35	11·7	50	Pt	200	0·23 ± 0·03
H13	35	11·7	6	Pt	220	0·13 ± 0·02
H14	8·6	14·6	5	Pt§	200	0·13 ± 0·04
H15	8·6	14·6	10	Pt§	200	0·16 ± 0·04

† 0·0002 in. diameter wire used unless indicated otherwise.
‡ 0·00015 in. diameter tungsten wire.
§ 0·001 in. diameter pure reference grade platinum wire.

TABLE 1. Summary of heat transfer data.

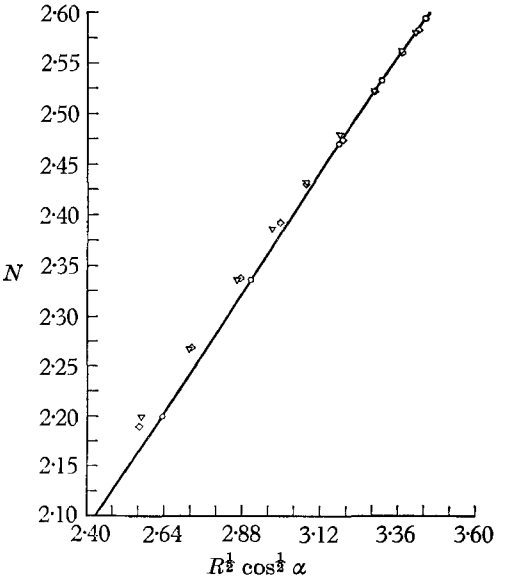

FIGURE 4. Variation of heat loss with normal component Reynolds number for various angles of yaw. Run 6: $(R)_\infty = 11{\cdot}7$; $U_\infty = 35$ m/s; $\ell/d = 200$ Pt wire; $a_w = 0{\cdot}80$; $k = 0{\cdot}22 \pm 0{\cdot}04$; ○, calibration data, $\alpha = 0°$; ◇, yawed wire ∠'s; ▽, yawed wire (−) ∠'s.

of the factor k. It is apparent that the deviations decrease with increasing wire length and represent an increase in the heat transfer rate for a yawed wire over that for a normal wire at the same value of $(R)_N$.

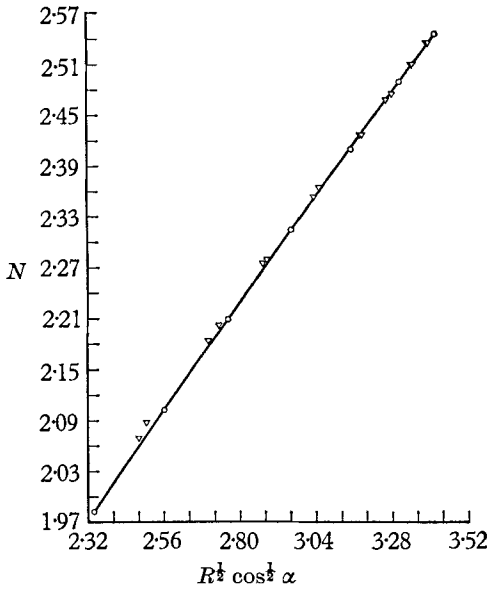

FIGURE 5. Variation of heat loss with normal component Reynolds number for various angles of yaw. Run 5: $(R)_\infty = 11{\cdot}7$; $U_\infty = 35$ m/s; $\ell/d = 450$ Pt wire; $a_w = 0{\cdot}80$; $k = 0{\cdot}10 \pm 0{\cdot}04$; ○, calibration data, $\alpha = 0°$; ▽, yawed wire data.

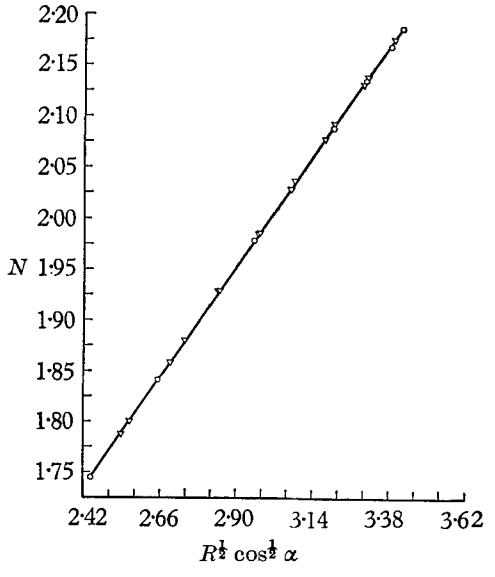

FIGURE 6. Variation of heat loss with normal component Reynolds number for various angles of yaw. Run 10: $(R)_\infty = 11{\cdot}7$; $U_\infty = 35$ m/s; $\ell/d = 600$ Pt wire; $a_w = 0{\cdot}80$; $k = 0{\cdot}00 \pm 0{\cdot}04$; ○, calibration data, $\alpha = 0{\cdot}80$; ▽, yawed wire data.

The magnitude of the increase in heat transfer for inclined wires over normal wires is quite small but is nevertheless detectable. The maximum increase occurred for the shortest wire used, $\ell/d = 200$, and at the largest angle of inclination. In the run H 6, for example, at $\alpha = 56° 3'$ the increase in heat loss is 1·4 %. This corresponds to an increase in bridge voltage of 0·7 % and gives some indication of the difficulty in obtaining data of this type.

For every run values of k were determined at each angle of inclination, and no correlation of k with α was indicated. The standard deviation of the values of k appears to be about $\pm$ 0·04 for each run.

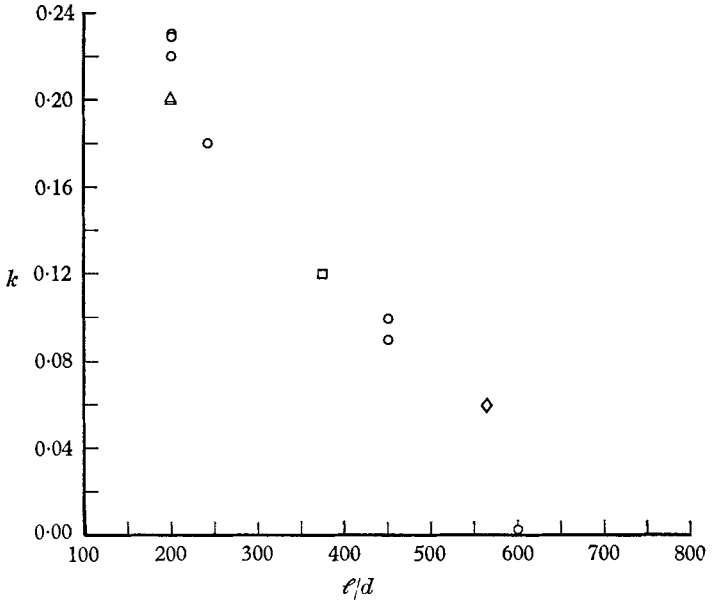

FIGURE 7. Dependence of k on ℓ/d. $(R)_\infty = 11{\cdot}7$; $U_\infty = 35$ m/s; $a_w = 0{\cdot}80$; ○, Pt wire, 5 μ diameter; □, W wire, 5 μ diameter; △, Pt-plated wire, 5 μ diameter; ◇, W wire, 3·8 μ diameter.

A series of runs was made to determine the effect of ℓ/d on the factor k. The Reynolds number, the mean temperature loading, and the wire material were kept the same, and only the ℓ/d parameter was varied. As shown in table 1, k was approximately 0·20 for a platinum wire with $\ell/d \approx 200$. As predicted, the value of k decreased as ℓ/d increased until at $\ell/d = 600$, k was essentially zero (see figure 7). The mean velocity, U_∞, used in these runs was 35 m/s, which gave a normal component Reynolds number based on the wire diameter of approximately 12. This is a favourable Reynolds number for these experiments as it is well above $R \approx 0{\cdot}1$, where free convection might become important (Collis & Williams 1959) and well below $R \approx 44$ where the onset of vortex shedding would occur.

The effect of the Reynolds number within a limited range was also investigated. Two runs were performed with the same hot-wire at the same temperature loading but with Reynolds numbers of 2·5 and 11·7 respectively. No significant effect on k was evident.

The temperature distribution on a platinum wire differs from that on a tungsten wire for a given ℓ/d, temperature loading, and Reynolds number because the thermal conductivity and temperature coefficients of resistivity are higher for tungsten than for platinum. No significant differences in k, however, are evident from the data.

Two kinds of hydrodynamic end effects were considered as possible explanations for the observed deviations from the cosine law. The first is the distortion of the flow field by the end supports, which causes flow acceleration across the wire near the upstream support and flow deceleration by the wire near the downstream support. Second is the development of the w-component of velocity near the upstream support, which would occur even in the absence of a support. This development, however, is not independent of the distortion caused by the supports, and the whole three-dimensional flow field is quite complex. The complexity of these two end effects precludes mathematical analysis and so each was studied experimentally.

The effect of flow-field distortion was investigated experimentally by varying the size as well as the geometry of the supports. Some wires, the tungsten and platinum-plated tungsten wires, had a section of copper plating on each end which removed the wire itself from the vicinity of the end supports. The length of the plated section was normally about 20 wire diameters. Such ends showed no observable effect on k. For platinum wires, ratios of the diameter of the support to the diameter of the wire, d_s/d_w, from 6 to 50 were tried while keeping the Reynolds number, the temperature loading, the ℓ/d ratio, and the wire material, platinum, the same. For d_s/d_w from 12 to 50 no significant differences in k could be determined. At $d_s/d_w = 6$, k was slightly smaller, but with such a small support this result could be attributed to a possible heating of the end support tips and a consequent reduction in the temperature non-uniformity along the wire.

Conclusions about the second kind of hydrodynamic end effect, axial development of the w-component, were drawn by analysis of certain runs. Study of the results from run H 6 for a $5\,\mu$, $\ell/\mathrm{d} = 200$ platinum wire show that the heat loss rate for the wire at 56° 3′ was $1{\cdot}084 \times 10^{-2}$ cal/s. The heat loss rate at $U(0)\cos 56°\,3'$ for normal component cooling was $1{\cdot}06 \times 10^{-2}$ cal/s, which indicates an increase of $0{\cdot}015 \times 10^{-2}$ cal/s above normal component cooling. If this increase were caused by w-component development effects, then it should remain constant as the wire length was increased, provided all other parameters remain constant and that the development of the w-component was complete before approximately 100 diameters, which is likely.

Consider now the following argument. The linearized equation governing the wire temperature distribution shows that the dimensional temperature distribution near the wire ends would be the same for the $\ell/d = 200$ and 600 wires if the parameters C_4/C_5, $C_5^{\frac{1}{2}}/\ell$ and $\tanh(\frac{1}{2}C_5^{\frac{1}{2}})$ of (20) were the same for both wires. Consideration of the constants C_4 and C_5 indicates that the first two conditions will hold if I is the same for both wires. The results of runs H 6 and H 10 show that I differs by about 5 % between the two wires and that C_5 is sufficiently large that $0{\cdot}998 \leqslant \tanh(\frac{1}{2}C_5^{\frac{1}{2}}) \leqslant 1{\cdot}000$ for the two wires. Thus the dimensional temperature

distribution near the wire ends should be approximately the same for both wires. Since the velocity field near the upstream wire end is the same for both wires, the heat loss rates near the upstream ends should be nearly the same for both wires. In other words, if a wire of $\ell/d = 600$ were made of the same wire material, had the same diameter, and operated at the same temperature loading, the same normal component Reynolds number, and the same angle of yaw, then the total heat loss should be about three times as great but the increase in heat loss over normal component cooling should be the same. Analysis of run H 10, which fulfills these requirements, shows that the heat loss rate is about 2·6 times that for the $\ell/d = 200$ wire, or $2{\cdot}623 \times 10^{-2}$ cal/s, at $\alpha = 55° 42'$. Thus, if one adds $0{\cdot}015 \times 10^{-2}$ cal/s to the heat loss rate for the $\ell/d = 600$ wire to account for the extra heat loss caused by the w-component development, the factor k is calculated to be 0·13. Since the value of k determined experimentally is $0 \pm 0{\cdot}04$, it appears that w-component development effects do not account for the increase in heat transfer for the yawed wire.

There remains the possibility that deviations from the cosine law can be attributed to a difference in the end conduction losses between normal and yawed wires. For an ℓ/d ratio of 200 the end conduction losses are of the order of 10 % of the total heat loss, so to account for the aforementioned 1·4 % increase, the total end conduction losses would have to increase by 14 %. To determine whether or not an increase of this magnitude occurred, wire temperature distribution measurements were required.

Since 0·001 in. wires were used in the temperature distribution measurements, heat transfer runs were made with them to ascertain that proper scaling of the probe was made. Run H 15 yielded $k = 0{\cdot}16 \pm 0{\cdot}04$, which compares well with the value of $0{\cdot}20 \pm 0{\cdot}04$ for the 5μ wires of the same value of ℓ/d. Temperature distribution measurements were, therefore, undertaken with wires of this diameter.

4.2. *Temperature distribution measurements*

Table 2 presents a summary of the temperature distribution measurements. The data from runs 4 and 5, plotted on figure 8, show the effect on the temperature distribution of yawing the wire with the normal component of velocity held constant. The temperature distribution on the inclined wire is asymmetrical, with the temperature maximum occurring at $\eta \approx 0{\cdot}4$.

Figure 9 shows that the measured end temperatures at the downstream end are linear to within 2–3 diameters from the support, whereas at the upstream end deviations appear at about 4 diameters from the support. These deviations were caused by solder or flux residue on the wire and, therefore, represent erroneous temperature determinations. The data show the temperature distribution to be nearly linear for 6–8 % of the wire length from the ends, and so the temperature gradients were obtained by placing a straight line through the data. The two or three readings nearest the end were ignored if they appeared to be abnormally high. The total end conduction loss for the normal wire was 7·9 %, while it was 8·0 % for the inclined wire, an increase of 1 %. The scatter in the end gradient data indicates that the smallest detectable difference in end conduction

loss is about 6 % for runs 4 and 5, runs 12 and 13, and runs 15 and 16. Thus the data are sufficiently consistent and precise to determine changes in end conduction loss that are smaller than the 14 % change required to explain the deviations

Run no.	ℓ/d	a_w	α (°)	U_∞ (m/s)	Gradients (°C/cm) Upstream	Gradients (°C/cm) Downstream	% end conduction loss	Mean T check (%)	d_s/d_w
1	200	0·8	0	8·61	—	—	—	8	10
2	200	0·8	0	5·42	—	—	—	8	10
3	200	0·8	50	†	—	—	—	8	10
4	202	0·8	0	5·55	$2{\cdot}36 \times 10^3$	$2{\cdot}41 \times 10^3$	7·9	12	20
5	202	0·8	55	†	$2{\cdot}36 \times 10^3$	$2{\cdot}48 \times 10^3$	8·0	12	20
6	197	0·8	0	5·41	—	—	—	—	S.E.‡
7	197	0·8	45	†	—	—	—	—	S.E.‡
8	400	0·8	0	5·45	$2{\cdot}36 \times 10^3$	$2{\cdot}39 \times 10^3$	4·1	8	20
9	400	9·8	50	†	$2{\cdot}54 \times 10^3$	$2{\cdot}53 \times 10^3$	4·3	8	20
10	400	0·8	0	8·57	$2{\cdot}19 \times 10^3$	$2{\cdot}31 \times 10^3$	3·3	9	20
11	400	0·5	0	8·57	$1{\cdot}92 \times 10^3$	$1{\cdot}57 \times 10^3$	4·6	16·7	20
12	199	0·8	0	5·06	$3{\cdot}03 \times 10^3$	$3{\cdot}11 \times 10^3$	9·9	8	S.E.
13	199	9·8	55	†	$2{\cdot}95 \times 10^3$	$3{\cdot}10 \times 10^3$	9·8	8	S.E.
14	199	0·5	0	4·98	$1{\cdot}37 \times 10^3$	$1{\cdot}51 \times 10^3$	7·3	14·1	S.E.
15	99	0·8	0	6·19	$3{\cdot}86 \times 10^3$	$3{\cdot}79 \times 10^3$	20·1	7	20
16	99	0·8	55	†	$3{\cdot}59 \times 10^3$	$3{\cdot}94 \times 10^3$	20·1	7	20
17	218	0·8	45	Probe 8·85	$2{\cdot}75 \times 10^3$	$2{\cdot}85 \times 10^3$	7·8	5	S.E.
18	199	0·8	45	8·75§	$2{\cdot}95 \times 10^3$	$3{\cdot}07 \times 10^3$	8·8	8	S.E.
19	199	0·8	30	8·75§	$3{\cdot}03 \times 10^3$	$3{\cdot}27 \times 10^3$	8·7	8	S.E.
20	400	0·8	0	5·20	$2{\cdot}19 \times 10^3$	$2{\cdot}31 \times 10^3$	4·0	9	20

† For inclined wire, wire voltage and resistance was maintained at $\alpha = 0°$ values.
‡ S.E. stands for special end as described in text.
§ Exceptions to a, as U_∞ for run 13 was 8·40 m/s.

TABLE 2. Summary of temperature distribution data.

from the cosine law for the $\ell/d = 200$ wire. Therefore, these results answer the question posed previously; deviations from the cosine law cannot be caused by the inclined wire having a higher end conduction loss than the normal wire. The increase in heat transfer from an inclined wire is caused by an increase in the convection loss and not by an increase in the end conduction loss, although more data were required to verify this conclusion.

A probe of $\ell/d = 199$ with special ends to simulate Wollaston wire and to determine the locations of the wire ends more accurately was used for runs 12, 13, 14, 18 and 19. Runs 12 and 13 were taken at $\alpha = 0°$ and $\alpha = 55°$, respectively, and the results were virtually identical in all respects to those of runs 4 and 5. Thus the data on the probe with the special ends confirms the conclusion that conduction loss cannot account for the increase in heat transfer displayed by inclined wires.

Also shown in figure 8 are the results of the numerical solution to (16) for run 4.

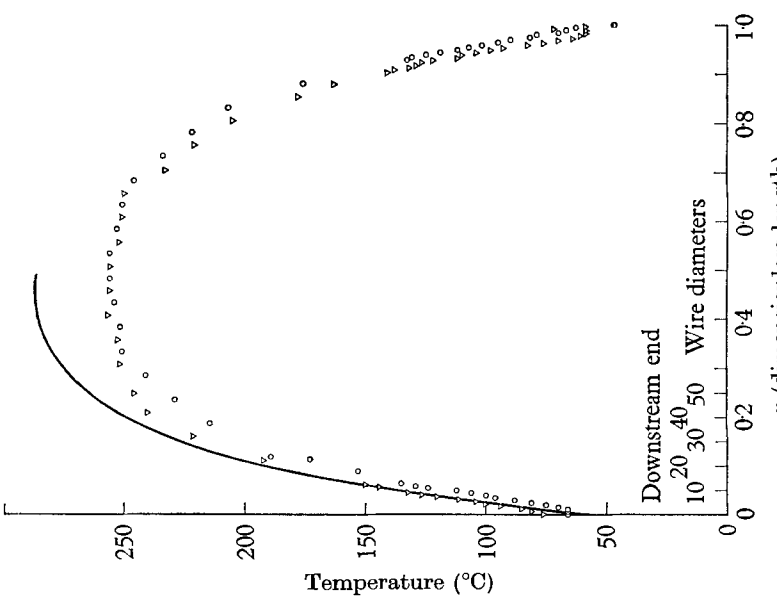

FIGURE 8. Temperature distributions along a $\ell/d = 202$ wire. $a_w \approx 0{\cdot}8$; $(R)_N = 9{\cdot}4$. ——, calculation; ○, run 4, $\alpha = 0°$; ▽, run 5, $\alpha = 55°$.

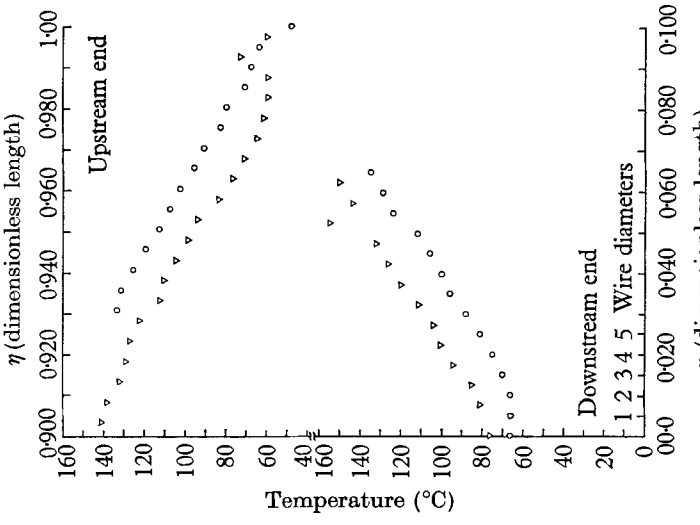

FIGURE 9. Temperature distributions at wire ends, $\ell/d = 202$; $a_w \approx 0{\cdot}8$; $(R)_N = 9{\cdot}4$. ○, run 4, $\alpha = 0°$; ▽, run 5, $\alpha = 55°$.

The parameters ℓ/d, U, T_a, I, R_a, R_w and $\Theta(0)$ from run 4 served as input data. The calculated temperature distribution agrees in shape with the experimental distribution quite well, although it gives temperatures on the order of 10 % higher in the middle of the wire. The calculated end conduction loss is 13·9 %, which is higher than the experimental value. The calculated end conduction loss could not be expected to agree precisely with the experimental value, however, as the effect of the flow field distortion caused by the end supports was not taken into account in the convection loss term. It should be mentioned that the solution of the linearized problem, (20), gives centre temperatures on the order of 100 °C higher than the experimental values.

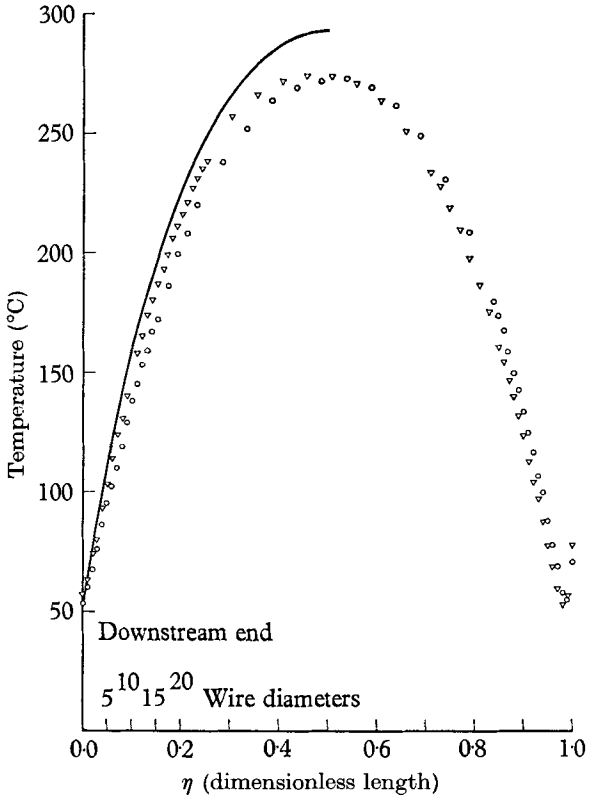

FIGURE 10. Temperature distributions along a $\ell/d = 99$ wire. $(R)_N = 10{\cdot}5$; $a_w \approx 0{\cdot}8$. ——, calculation; ○, run 15, $\alpha = 0°$; ▽, run 16, $\alpha = 55°$.

A probe with $\ell/d = 99$ was constructed to determine how peaked the temperature distribution might become for such a short wire. Figure 10 shows the results from runs 15 and 16, which were carried out using this probe. The temperature maximum is shifted to $\eta \approx 0{\cdot}45$ for the wire inclined at $\alpha = 55°$. The end gradients are shown in figure 11, and the end conduction losses were 20·1 % for both the normal and inclined wires, which again indicates no effect of yaw. The computed temperature distribution for run 15 is shown in figure 10. The calculated end conduction loss was 27·5 %.

Figure 12 shows the results of runs 10, 11 and 20 for the same $\ell/d = 400$ hot-

wire probe. In runs 10 and 11 the velocity was the same but the overheat ratio was changed. Note that a large portion of the wire, $0{\cdot}2 < \eta < 0{\cdot}8$, is at an approximately uniform temperature. Run 20, with $U_\infty = 5{\cdot}20$ m/s, was taken 9 days after run 10 was performed. The lower velocity gives slightly higher temperatures

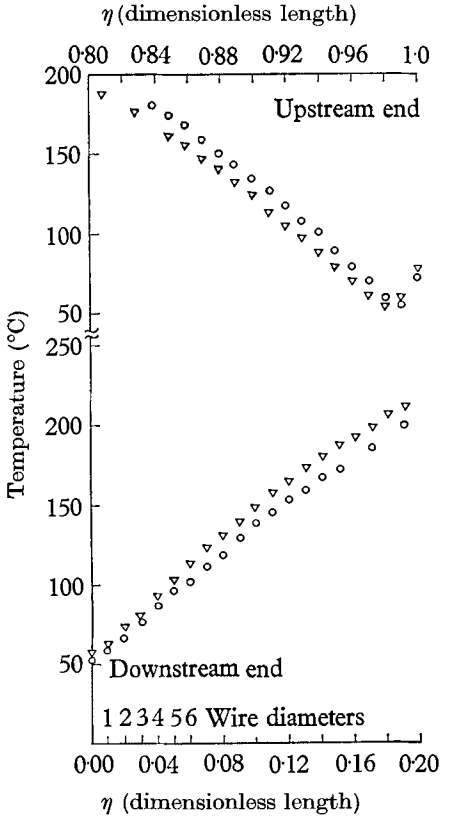

FIGURE 11. Temperature distributions at wire ends, $\ell/d = 99$; $a_w \approx 0{\cdot}8$; $(R)_N = 10{\cdot}5$. ○, run 15, $\alpha = 0°$; ▽, run 16, $\alpha = 55°$.

near the middle of the wire, but near the ends the temperature distributions coincide. Also shown in figure 12 is the computer distribution for run 20. The calculated end conduction loss is 6·7 % as compared to the experimental value of 4·0 %.

It is interesting to note that when the wire overheat ratio was 0·8, the temperatures of the wire ends were considerably higher than the static temperature of the stream, which was about 23 °C for most of the runs. The temperatures approached 50–60 °C for $\alpha = 0°$ and were about 60–70 °C at the downstream end and about 40 °C at the upstream end for the inclined wire. These results are for probes with $d_s/d_w = 20$. The reason for these differences and the asymmetry of the temperature distribution could be the result of the hydrodynamic end effects or the effects of the w-component of velocity or both. No detailed attempt to determine which, if any, of the above effects were prevalent, although a 45° probe (with the needles parallel to the flow) was made to determine whether the

temperature distribution might be affected by the different flow field over such supports. This probe simulated one wire of an X-array more closely than the probes used in other runs. The temperature distribution on this wire was found to be quite similar to that on the other inclined wires.

An indication of the accuracy of the temperature measurements can be obtained by comparing the mean temperature of the wire obtained by integration of the temperature distribution with that obtained from the temperature

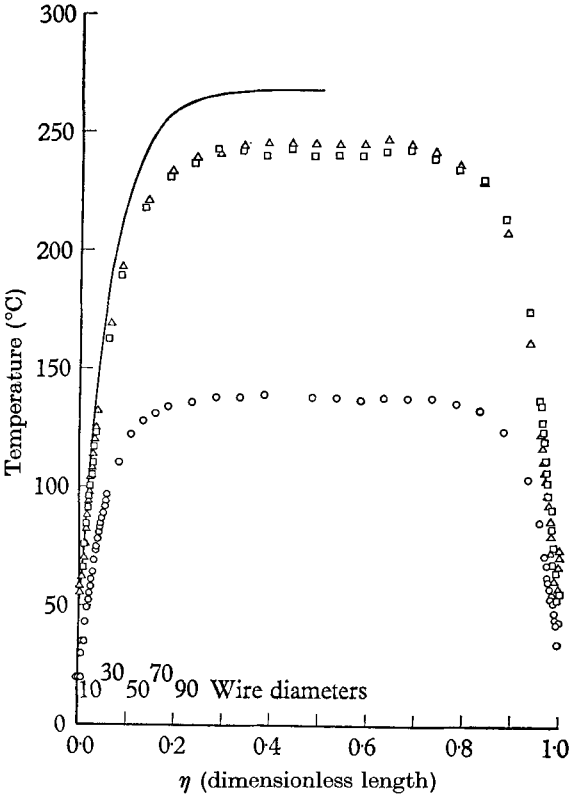

FIGURE 12. Temperature distributions along a $\ell/d = 400$ wire for two different velocities and overheat ratios. $\alpha = 0°$. ——, calculation, run 20; □, $a_w \approx 0{\cdot}8$, $U_\infty = 8{\cdot}57$ m/s, run 10; ○, $a_w \approx 0{\cdot}5$, $U_\infty = 8{\cdot}57$ m/s, run 11; △, $a_w \approx 0{\cdot}8$, $U_\infty = 5{\cdot}20$ m/s, run 20.

coefficient of resistance and the overheat ratio of the wire. The overheat ratio of the wire is known to within approximately ± 3 %, and thus the mean temperature can be determined to within about ± 3 %. The mean temperature so measured was usually about 10 % higher than the value calculated from the measured temperature distribution, as indicated under 'mean T check' in table 2. For the low overheat cases the disagreement was slightly larger. The good agreement between the two determinations confirm that the assumptions made in the interpretation of the infra-red radiometer readings are reasonable.

It is difficult to assess the accuracy of each temperature measurement because of the temperature dependent sensitivity of the infra-red detector and possible

small differences between the emissivities of the calibration surface and the wire surfaces. We believe, however, that the accuracy of the temperature measurements is approximately the same at all temperatures. In particular, much confidence can be placed upon the comparisons between the end temperature gradients for yawed and normal wires since the data were taken on the same wire and interpreted with the same calibration curve.

5. Conclusions

The results of the heat transfer and temperature distribution measurements indicate that inclined hot-wires are sensitive to the tangential velocity component along the wire. For the range of Reynolds number investigated, $2 < R < 15$, the degree of sensitivity can be expressed by the factor k in the relationship for the effective cooling velocity:

$$U^2(\alpha) = U^2(0)\,(\cos^2\alpha + k^2 \sin^2\alpha).$$

k depends on the parameters that govern the temperature distribution along the wire, primarily the length-to-diameter ratio of the wire. For a platinum wire of $\ell/d \approx 200$, $k \approx 0{\cdot}2$ and decreases with increasing values of ℓ/d until at an $\ell/d = 600$ it is essentially zero.

The temperature distribution measurements indicate that inclined and normal wires have nearly identical end conduction losses, although the temperature distribution on an inclined wire is asymmetrical. Therefore, the deviation from the cosine law is caused by an increase in the convection heat loss attributable to the tangential component of velocity.

The sensitivity of an inclined hot-wire to the tangential velocity component must be taken into consideration when interpreting hot-wire data in terms of velocity components of a flow field. Hot-wire response equations which include the effects of the tangential velocity component as well as the nonlinearities caused by high intensity turbulence are presented in part 2 of this paper.

The authors are grateful to Mr Robert W. Boice, who with skill and great care built the hot-wire probes for this study. We would also like to express our appreciation to Mr Truman W. Nybakken for his assistance in improving the thermal sensitivity of the intra-red detector, and to Mr John L. Lundeberg for his assistance in constructing various parts of the equipment. Thanks are also due to Mr William C. Cook for his help with the computer programming.

REFERENCES

Betchov, R. 1952 *NACA Tech. Memo.* no. 1346.

Champagne, F. H. 1966 Ph.D. Dissertation, University of Washington.

Champagne, F. H. & Lundberg, J. L. 1966 *Rev. Sci. Instr.* **37**, 838.

Chu, W. T. 1964 *Ann. Prog. Rep., Inst. for Aerospace Studies, Univ. of Toronto*, no. 42.

Collis, D. C. 1956 *J. Aero. Sci.* **23**, 697.

Collis, D. C. & Williams, M. J. 1959 *J. Fluid Mech.* **6**, 357.

Corrsin, S. 1963 *Encyclopedia of Physics*, 1st ed., vol. viii/2, 555. Berlin: Springer-Verlag.

Davies, P. O. A. L. & Fisher, M. J. 1964 *Proc. Roy. Soc.* A **280**, 486.

DELLEUR, J. 1964 *C.R. Acad. Sci., Paris*, **269**, 712.

HINZE, J. O. 1959 *Turbulence*, 1st ed., chap. 2. New York: McGraw-Hill.

JONES, R. T. 1947 *NACA Tech. Note*, no. 1402.

KING, L. V. 1914 *Phil. Trans.* A **214**, 373.

KRONAUER, R. E. 1953 *Pratt and Whitney Res. Rept.* no. 137.

NEWMAN, B. G. & LEARY, B. G. 1950 *Aero. Res. Lab. Rep.* A 72. Department of Supply, Australia.

PRANDTL, L. 1946 *Ministry of Aircraft Production Völkenrode, Rept. and Trans.* no. 64.

SANDBORN, V. A. & LAURENCE, J. C. 1955 *NACA Tech. Note*, no. 3563.

SCHOLLMEYER, H. 1965 *Proc. of the Aerodynamic Inst., Aachen*, no. 18, 33.

SCHUBAUER, G. B. & KLEBANOFF, P. S. 1946 *NACA Adv. Conf. Rept.* no. 5K27, Wartime Report W-86.

SEARS, W. R. 1948 *J. Aero. Sci.* **15**, 49.

SEARS, W. R. 1954 *Appl. Mech. Rev.* **7**, 281.

WEBSTER, C. A. G. 1962 *J. Fluid Mech.* **13**, 307.

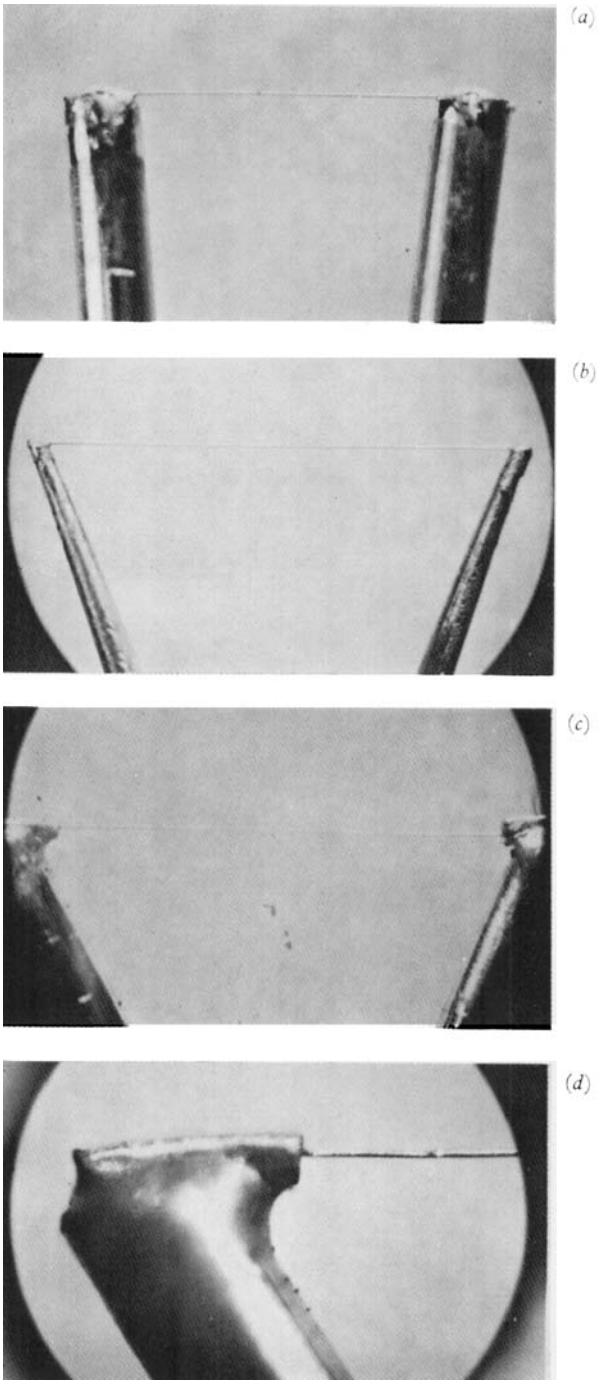

FIGURE 2. Photograph of 1 mil diameter platinum wires. (*a*) $\ell/d = 99$ wire; $d_s/d_w \approx 20$. (*b*) $\ell/d = 100$; $d_s/d_w \approx 10$. (*c*) $\ell/d = 199$; special end (note: r.h.s. end was deformed in placing and removing thermocouple). (*d*) Close-up of special end for $\ell/d = 199$ probe.

CHAMPAGNE, SLEICHER AND WEHRMANN (*Facing p.* 176)